The Promotion by Steam on CaO Adsorbing SeO_2 at Medium Temperature

Yu Lou[1], Yaming Fan[1], Chengkai Pang[1], and Yuqun Zhuo[1]

1 Department of Energy and Power Engineering, Tsinghua University, Beijing 100084, China.
E-mail: louy15@mails.tsinghua.edu.cn

Abstract. This study investigated the promotion of steam for CaO adsorbing SeO_2 gas at the medium temperature interval (240℃-800℃), based on the previous studies on CaO adsorbing SeO_2 gas. The experiments revealed both the influences of temperature and steam concentration. The mechanism of the promotion is similar to those of steam in carbonation and is confirmed by a series of designed experiments and characterization of the products of gaseous SeO_2 adsorption.

1. Introduction

Selenium is an important industrial material used in many fields, such as electronics, metallurgy and petrochemical [1]. Although selenium is a necessary trace mineral elements for human beings, excessive intake damages health [2]. The toxicity of selenium compounds varies with the different kinds, both selenite and seleninic acid are highly toxic, which usually come from selenium dioxide [3]. Selenium was generally considered as a dispersive element, whose concentration is only 0.05-0.09 μg/g in lithosphere [4]. However, there is one kind of stone coal in Enshi region, Hubei Province, P. R. China, which contains 80000 μg/g selenium [5]. According to previous researches, coal was adjudged as one important selenium enrichment and the main emission source [6], [7]. In 1995, the selenium emission caused by fossil fuel (mostly coal) combustion reached 4101 tones, more than 89 percent of total anthropogenic emissions [8]. Tian et al. counted 787 tons of the selenium emission resulted from coal-fired power plants in 2007 in China [7].

With the increasing environmental awareness, controlling selenium emission has become more and more important. Since 1998, US EPA has set selenium as one of which needs to be monitored among coal-fired power plant emissions [9], [10]. On Dec. 2011, US EPA announced "Mercury and Air Toxics Standards" (MATS), which contained the emission limits of various power plants' pollutants, including selenium, and updated in March 2016.

Many researches have focused on adsorption reactions to reduce selenium emission [11]-[15]. A. Ghosh-Dastidar et al. have researched several minerals as adsorbent to gaseous SeO_2 at 500℃ and 900℃, including limestone, kaolin, alumina and calcium carbonate. The results of adsorption reactions proved that CaO was the best adsorbent to deal with SeO_2, and the process was chemical adsorption leading to the product of $CaSeO_3$ [14]. Other studies used the mixture of CaO and selenium-containing substances, which also suggested that CaO was very reactive with selenium [13], [16].

Meanwhile, the reactivity of CaO affected by steam, whether physically or chemically, has been investigated for a long time. As early as 1977, Dobner et al. found that steam could "catalyze" CaO adsorbing CO_2 (carbonation) on 550℃ [17], suggesting that if there was steam at certain flow-rate at 550℃, it would significantly increase for the adsorption rate and extent of carbonation when

compared with the results of no steam. Some researchers have proved that steam can improve the effect of calcium looping and adsorption efficiency of carbonation [18]-[20]. V. Manovic investigated 8 kinds of limestone at different temperature (350℃-800℃) and found the promotion from steam on carbonation was more obvious under relatively low temperature (below 600℃) [19], similar to other research [21].

The mechanism of promotion was proposed by previous researches that the key step was the dissociative of H_2O molecule on the surface of CaO solid, depending on the oxygen vacancies of the surface of CaO [22], [23], described by (1):

$$H_2O(g) + Vo + Oo = 2OHo \tag{1}$$

The products of this process, i.e. hydroxyl groups on oxygen site have been regarded as the crux of carbonation. The total energy of dissociative adsorption can be expressed by (2). J. Carrasco et al., H. Manzano et al., and D. Ochs et al. have pointed out that the $E_{H2O,\,diss,\,ad}$ is smaller than $E_{H2O,\,ad}$ [24]-[26], which is regarded as the most important part of the proposed mechanism. Although there are some theoretical and experimental implications support this mechanism [22], [23], the direct evidence, especially the evidence from experiments, are generally absent.

$$E_{H_2O,diss,ad} = E_{OH,ad} + E_{H,ad} - E_{H_2O,diss} \tag{2}$$

Due to similar molecule structure with CO_2, it is also very interesting to see if the adsorption of SeO_2 on CaO could be promoted by steam in similar temperature interval (300℃-800℃). CaO, which possesses massive advantages of low cost, wide availability and non-toxic, has been widely used in desulphurization processes. It would be beneficial for power plants to remove multiple contaminants in a single process. Therefore, to understand the influence and mechanism of steam on CaO adsorbing gaseous SeO_2 is of great interests. In this study, both experimental and products characterization analysis have adopted to reveal the interactions among CaO, SeO_2 and H_2O.

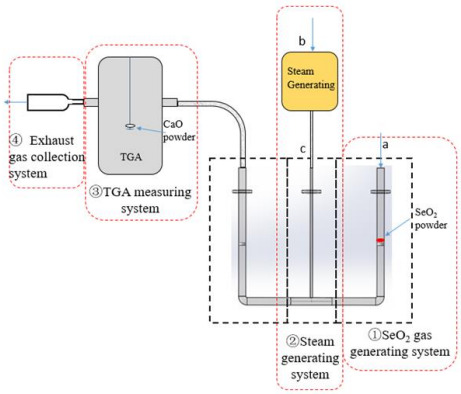

Figure 1. Schematic of SeO_2 adsorption.

2. SeO_2 Adsorption Experiments

2.1. Assemblies

The experimental assembly of SeO_2 adsorption on CaO solid consists of four sub-systems as shown in Figure 1, which are SeO_2 gas generating system, steam generating, TGA(Thermal Gravimetric Analyzer) measuring, and exhaust gas collection. The main reactor includes a three section resistance-heating furnace and TGA (Thermal Gravimetric Analyzer). SeO_2 gas generating system is an improved mimic of the device established by Li et al [11], and Sterling et al [27]. Gaseous SeO_2 is generated in the first section of furnace, in which analytic pure SeO_2 powder is placed on an internal sieve plate. Gaseous SeO_2 is sublimated by controlling the heating temperature, and is carried out by pure nitrogen. Steam generating system located in the second section of furnace consists of an injection pump, a metal furnace. The generated steam is mixed with pure nitrogen and SeO_2 gas at above 250℃ in the second and third sections. Analytic pure CaO powder is placed on a platinum plate,

which hangs in a 22mm (inner diameter) quartz tube in TGA. Exhaust gas collection system is a specially designed quartz tube with the purpose to collect all escaped SeO_2 by condensation.

2.2. Material

Analytic pure SeO_2 and CaO solid are used as vapor source and adsorbent respectively in these experiments. The desired SeO_2 concentration in gas can be attained by adjusting the temperature of vapor generator. The balance gas is pure N_2. As calibrated previously, the temperature and N_2 carrier flow rate have been set at 190℃ and 100ml/min, which maintains the SeO_2 concentration at 40ppm in mixed gas [14], [15].

2.3. Steps for without-steam experiments

N_2 purging was used as the step of Pretreatment Ⅰ for all experiments. CaO sample was preheated to 800℃ and held for 5 min. in pure N_2 to remove water and other volatile impurities. Then, the CaO sample was cooled to the set experimental temperature. The analytic pure SeO_2 sample was placed on a sieve plate of the first section in furnace, where the temperature was maintained at 190℃. For without-steam experiments, continuous measurement method was adopted under various temperatures, i.e. 7 temperature stages within 240℃-800℃ range, as shown in Figure 2. The CaO temperature was first set to 800℃ for SeO_2 gas adsorbing as the first stage, and then gradually cooled to 240℃ as the 7th stage. After the last stage (240℃), CaO sample was heated up to 400℃ and 800℃ to see if it maintained the same adsorption activity as the former stages throughout the whole process.

2.4. Steps for with-steam experiments

Pretreatment Ⅰ and similar processes after that were also used. CaO sample was cooled to and maintained at desired temperature stage. Then the steam generating system was turned on and SeO_2 powder was simultaneously placed in. Each with-steam adsorption test was held for 20 min. Due to the simultaneous adsorption of steam and SeO_2 on CaO sample, the adsorbed quantity of selenium has to be determined by ICP-AES. According to previous researches [11], [12], CaO solid could stably adsorb gaseous SeO_2 under experimental conditions for hours. Therefore, the adsorption rate could been considered as constant during the whole adsorption process.

2.5. Reliability

For without-steam experiments, as continuous measurement had been conducted at various temperature, the reliability of experimental data was verified by the deviation of multiple repeated runs. The relative experimental error range has been determined as ±5%. For with-steam experiments, the reliability of experimental data was affirmed by selenium balance across the whole system. The selenium balance was established by: 1) After stopping the SeO_2 generating furnace and taking out the adsorption product from TGA, place fresh CaO powder into reactor; 2) Restart the SeO_2 generating furnace to evaporate the rest SeO_2; 3) Collect the later placed CaO solid and rinse the exhaust gas collection system, by which means all remaining SeO_2 could be collected and later determined by ICP-AES. Some of the selenium balance are shown in Table 1. The relative experimental error range for experimental data from with-steam tests was determined as ±3%.

Table 1 Selenium Balance Measuring (part experiments)

Experiments	Total SeO_2(μg)	SeO_2□ (μg)	SeO_2□ (μg)	Balance
400□-6%H_2O Adsorption	1.23×10^4	3.42×10^2	1.16×10^4	0.983
320□-20%H_2O Adsorption	1.05×10^4	2.55×10^2	9.99×10^3	0.972

2.6. Results and discussion

For without-steam experiments, the SeO_2 adsorption rates are shown in Figure 2. The data from unstable periods due to temperature adjusting had been removed. Only the CaO weight increase within the 5-10 min of temperature-stable segment were presented. The adsorption rates of the last two segments (400℃ and 800℃) of the series agreed well with the previous rates under corresponding

temperature, suggesting the CaO adsorption activity was not affected by either temperature or adsorption itself.

The results of without-steam experiments shows that from 240℃ to 800℃, the SeO_2 adsorption rate rises with the increment of adsorption temperature, and the maximum reaches about 21μg/min at 800℃. It is necessary to point out that both SeO_2 desorption and the activity of SeO_2 adsorption sites on CaO surface increases with increasing temperature. The results clearly indicates that the influence of the latter is more predominant in this atmosphere. What the experiments shows complies with previous research to a certain degree. Ghosh-Dastida et al. found SeO_2 adsorption rate on CaO increased at 400℃—600℃, though in the atmosphere of 5% O_2 + 95% N_2 [14]. Li also found similar SeO_2 adsorption results at 300℃—400℃, though in another atmosphere – air [11].

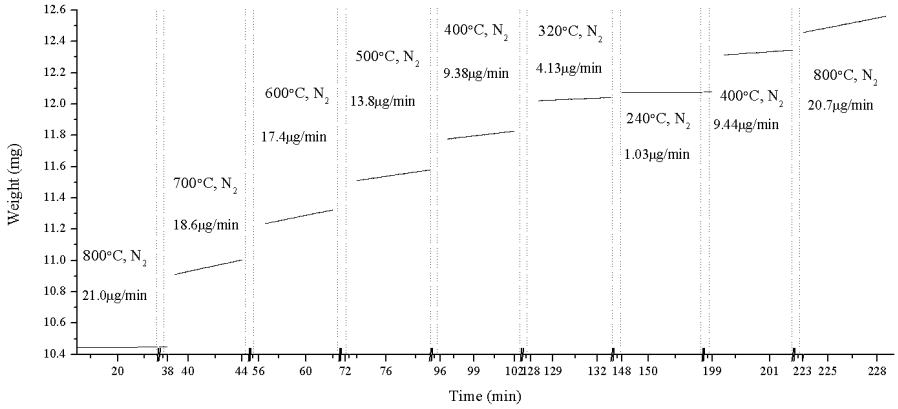

Figure 2. 240℃-800℃ without-steam SeO_2 adsorption rate.

For with-steam experiments, the adsorption rate for SeO_2 is influenced by both the steam concentration and adsorption temperature, as shown in Table 2 and Figure 3 a). In Table 2, the adsorption temperature was set to 400℃, and the actual quantity of SeO_2 adsorbed on CaO was determined by ICP-AES. As mentioned above, the SeO_2 adsorption rate on CaO would be stable for a relative long period, thus it is safe to assume that the adsorption rate of the same condition would remain stable in experiment. The SeO_2 adsorption rate could be calculated from the ratio of adsorption quantity and adsorption time as shown in (3).

$$R = W_{SeO_2} / \tau \tag{3}$$

Table 2. SeO_2 Adsorption rate influenced by steam concentration

C_{H_2O}(%)	W_0(μg)	W'(μg)	W_i(μg)	W_{SeO_2} (μg)	R (μg/min)
0	9.77×10^3	9.97×10^3	2.01×10^2	2.01×10^2	9.82
6	9.79×10^3	1.01×10^4	4.11×10^2	3.40×10^2	17.1
10	9.39×10^3	9.90×10^3	5.10×10^2	3.71×10^2	18.7
16	9.68×10^3	1.03×10^4	5.82×10^2	4.02×10^2	19.8
20	9.89×10^3	1.06×10^4	7.20×10^2	4.11×10^2	20.4

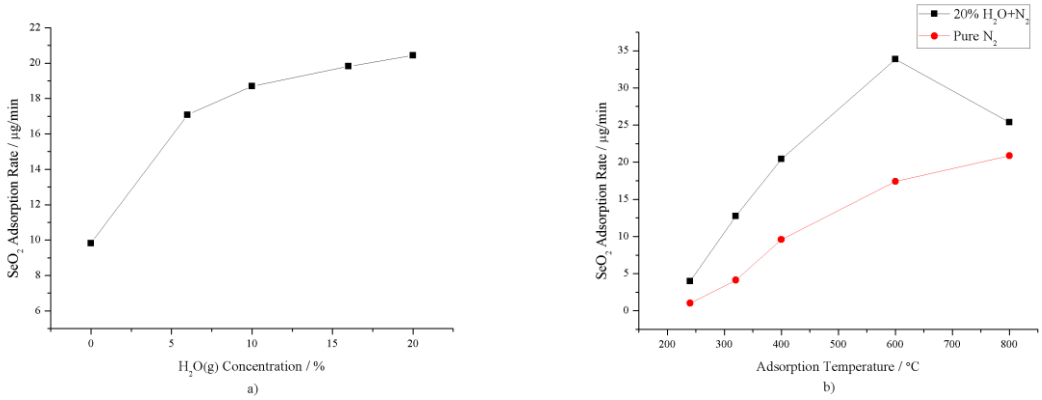

Figure 3. a) SeO_2 adsorption rate influenced by steam concentration; b) SeO_2 adsorption rate influenced by adsorption temperature.

As shown in Figure 3 a) and Table 2, steam (concentration up to 20%) can promote CaO adsorbing SeO_2 at 400℃, which is positively related with the steam concentration. The results also indicates that the promotion of the steam slows down along with the increment of steam concentration. When the steam concentration is above 10%, the adsorption rate is approaching its maximum, slightly above 20μg/min. Further increasing the steam concentration may not increase the adsorption notably.

Table 3. SeO_2 Adsorption rate influenced by adsorption temperature (with-steam experiments)

T(℃)	W_0(μg)	W'(μg)	W_i(μg)	W_{SeO2} (μg)	R (μg/min)	R_0(μg/min)
240	1.01×10^4	1.07×10^4	5.61×10^2	0.081	3.97	1.03
320	9.05×10^3	9.54×10^3	4.90×10^2	0.262	12.8	4.13
400	9.89×10^3	1.06×10^4	7.22×10^2	0.411	20.4	9.59
600	8.81×10^3	9.51×10^3	7.13×10^2	0.680	33.9	17.4
800	8.83×10^3	9.33×10^3	5.10×10^2	0.510	25.4	20.9

The influence of the temperature on SeO_2 adsorption is shown in Table 3 and Figure 3 b). The experimental conditions were similar as before. The steam concentration was set to 20% for better demonstration. The SeO_2 adsorption rates without steam are also shown in the table and figure for comparison purposes.

As shown in Figure 3 b), there is an obvious promotion for CaO adsorbing SeO_2 gas in 240℃-800℃ with 20% steam, comparing with no steam at same temperature. There is a peak at 600℃ for the fastest SeO_2 adsorption rate, about 33.85 μg/min. Before this peak in Figure 3 b), the rate rises along temperature, similar to those experiments without steam. After the peak (about 600℃), however, an inverse trend of SeO_2 adsorption rate appears (without steam). This could be explained by the diminishing of the steam adsorption ability on CaO surface along with temperature, which has been discussed by other researchers in carbonation study [19], [21].

As mentioned before, the dissociation of chemisorbed H_2O molecule on CaO solid surface could be the key to understand how steam promote CaO adsorbing CO_2. Due to similar molecular structure and reaction phenomenon, this reaction path could be also applied to explain the steam promotion of SeO_2 adsorption on CaO. In this mechanism, the oxygen vacancies on CaO solid surface are regarded as the crux of the dissociation of chemisorbed H_2O molecule. The product of H_2O molecular reaction on CaO surface is a significant factor affecting SeO_2 adsorption. Combined with the findings in previous [22], [23] and the experimental results from this study, the mechanism of steam promoting CaO adsorbing SeO_2 is illustrated in Figure 4.

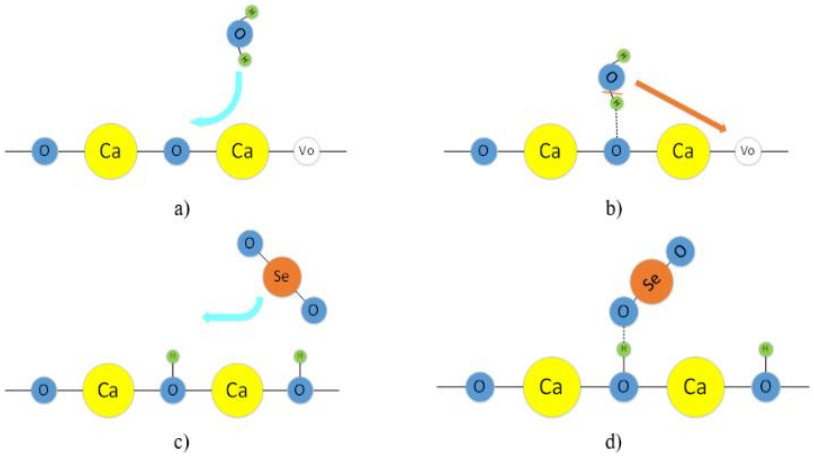

Figure 4. Schematic diagram for steam promoting CaO solid adsorbing SeO_2 gas. a) H_2O molecule adsorbed on an oxygen site on CaO surface; b) adsorbed H_2O molecule dissociated to adjacent oxygen vacancies on CaO surface, forming two hydroxyl groups; c) CaO surface with hydroxyl groups formed from H_2O molecule attracts SeO_2 molecule; d) the possible SeO_2 adsorption state on CaO surface with hydroxyl group.

As shown in Figure 4, the hydroxyl groups formed from H_2O molecule is essential for SeO_2 adsorption. However, what presented in Figure 4 was still an assumption at this stage. Due to the difficulties in direct observation of CaO surface, experiments were designed to verify step a) and b), and some characterization analysis focusing on the reaction products was employed to support step c) and d).

3. Experiments: H_2O Dissociation on Oxygen Sites/Vacancies

To confirm the role of oxygen sites/vacancies on CaO surface in H_2O dissociation [22], [23], an experimental rig was constructed as shown in Figure 5. By purging the CaO sample by a certain concentration of CO in advance, the amount of oxygen sites/vacancies on CaO surface could be qualitatively changed and the later reaction rate of ($CaO(s) + H_2O(g)$) could be adjusted accordingly. The reaction rate of kinetic-controlled stage represents the chemical change of CaO surface directly, and could be used to reflect the change of oxygen sites/vacancies. Although there is hardly any research focusing on how CO could change the CaO surface, some studies concerning the change of surface oxygen sites of metallic oxide by CO could be helpful [28]-[30].

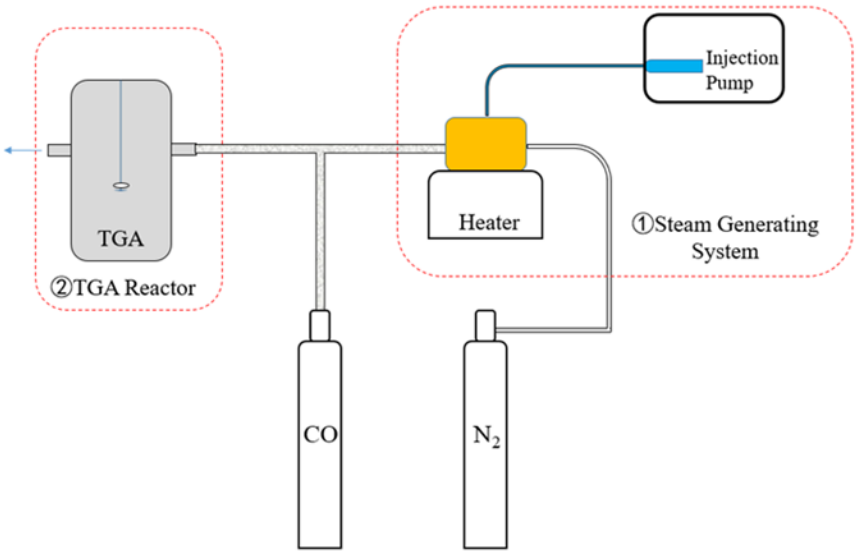

Figure 5. Schematic for CaO (s) + H_2O (g) after CO Modification.

3.1. Assemblies:
The experiment bench includes steam generating system and TGA reactor, similar as before.

3.2. Material
The same analytic pure CaO was used. CO concentration (2000ppm and 10%) was maintained by mass flow controllers. The gas mixture was balanced by N_2 and the total gas flow is 100ml/min.

3.3. Steps
For the same reasons as before, 800℃ N_2 purging as Pretreatment Ⅰ was adopted firstly. Then the CaO sample was cooled to the CO-pretreatment temperature, during which CaO surface was purged by CO for 20 min. This step was Pretreatment Ⅱ. Various temperatures and CO concentrations were chosen in Pretreatment Ⅱ. After this step, another pretreatment was used to ensure that no CO adhered on CaO surface, i.e. Pretreatment Ⅲ, in which CaO sample was heated to 800℃ again and held for 5 min. in pure N_2. After all pretreatments, CaO sample was cooled to the reaction temperature of 320℃. The different reaction rates were measured by TGA. The pressure in the reactor during the whole series of experiments was kept atmospheric.

3.4. Results and discussion
After Pretreatment Ⅱ, the reaction rates of ($CaO(s) + H_2O(g)$) varied obviously as shown in Figure 6 and Figure 7. In each a) part of the two figures, experimental data and both horizontal and vertical coordinates have been normalized, which means the percentage data was shown in the figure instead of actual weight variation to eliminating small weight differences between different sample. The zero of horizontal coordinates represents 5 min before the reaction beginning. For the vertical coordinates, the original weight means the sample weight after 800℃ N_2 purging (Pretreatment Ⅱ). In each b) part of the two figures, the reaction rate means the reaction rate of kinetic controlled stage in a) part for different Pretreatment Ⅱ conditions.
Figure 6 represents the influence of different CO concentrations in pretreatment Ⅱ on reaction rate. The results demonstrated that the ($CaO(s) + H_2O(g)$) reaction rate increased notably after low CO concentration pretreatment, but decreased after high concentration pretreatment. If put into logarithmic horizontal coordinate as shown in Figure 6 b), it is obvious that the effect of CO concentration on reaction rate has a limit.
As shown in Figure 7, comparing with the data without CO, low temperature CO pretreatment enhanced the reaction rate of ($CaO(s)+H_2O(g)$). However, an inhibition in high temperature was also observed. The concentration of CO in Pretreatment Ⅱ was set to 250 ppm. In general, under these experimental conditions, the reaction rates decreased along with increasing temperature.

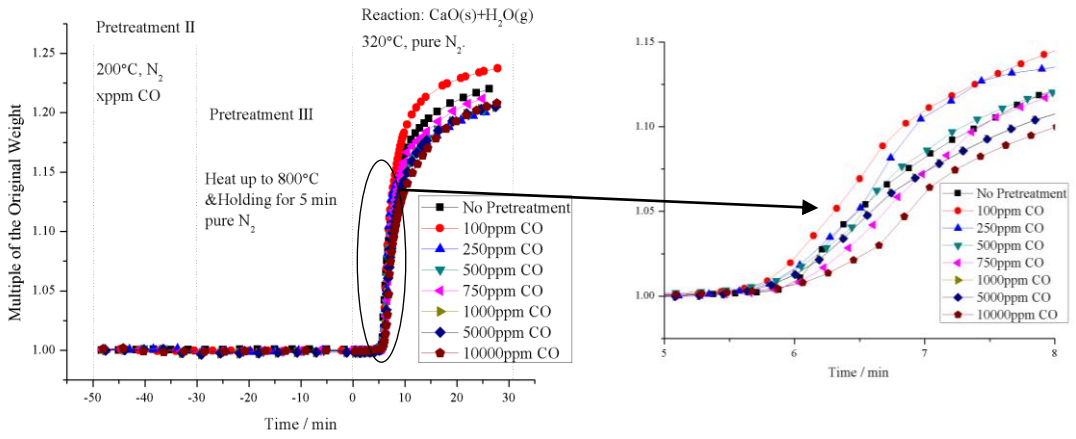

a)

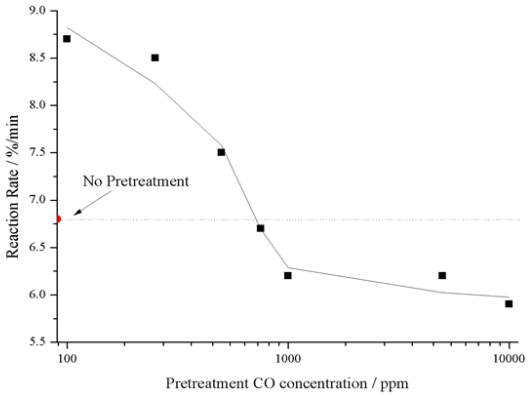

b)

Figure 6. The influence of CO concentration in Pretreatment Ⅱ on CaO(s) + H_2O(g) reaction.

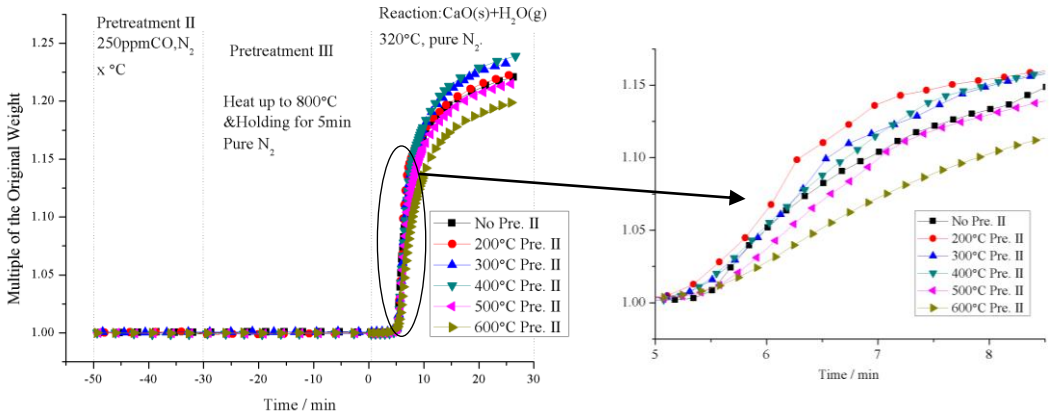

a)

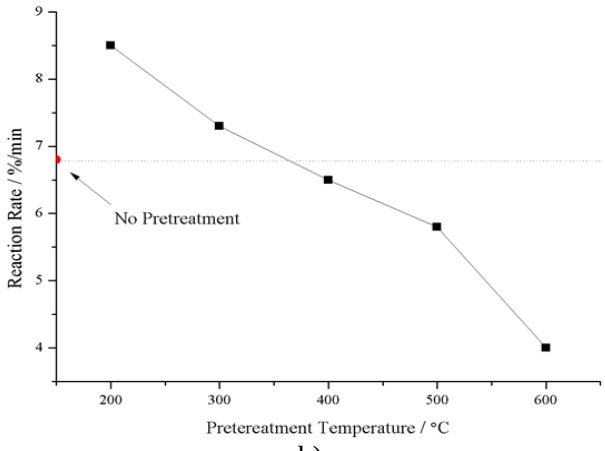

b)

Figure 7. The influence of CO concentration in Pretreatment Ⅱ on CaO(s) + H_2O(g) reaction.

It seems that there is coherence in the appearance of Figure 6 and Figure 7. When temperature or CO concentration in pretreatment rises, CO should have stronger effect on CaO surface. Comparing with no Pretreatment Ⅱ, both the two figures indicates it leads an inhibition on (CaO(s)+H_2O(g)) reaction rates if the temperature or CO concentration in Pretreatment Ⅱ exceeds a certain limits. However, an

obvious promotion on the rates could happen if the conditions in Pretreatment Ⅱ are relatively moderate, which means whether the pretreatment temperature or CO concentration is within the limits. This phenomenon would hardly been explained by CO adsorption in Pretreatment Ⅱ, due to no obvious weight change on TGA during in this process. Furthermore, Pretreatment Ⅲ was designed to ensure that there wasn't any CO adsorption on CaO surface after Pretreatment Ⅱ. As in the previous researches on steam promotion on CaO adsorbing CO_2, the most possible explanation for these results is that CO molecule changes the oxygen sites/vacancies during Pretreatment Ⅱ, which could be also regarded as the key of H_2O dissociation in Figure 4. H_2O molecule would first chemisorbs on oxygen site and then decomposes by the influence of adjacent oxygen vacancies. Due to the fact that $E_{H2O, diss, ad}$ is smaller than $E_{H2O, ad}$ as mentioned before, the CaO surface with relative more oxygen vacancies reduces the energy required for H_2O molecule adsorption. Fan et al. have investigated this situation through DFT method [31] and acquired the same conclusion. Comparing with oxygen sites on CaO surface, oxygen vacancies should be in minority. In Pretreatment Ⅱ, CO purging increases the amount of the oxygen vacancies and decrease the oxygen sites consequently. Whether low temperature or low CO concentration can only increase the oxygen vacancies to a finite extent, thus it makes the whole adsorption energy of H_2O molecule lower on CaO surface and promotes the reaction rate of $CaO(s)+H_2O(g)$. When temperature or CO concentration rises furthermore, oxygen vacancies increase and eventually becomes dominant on CaO surface. The amount of surface active oxygen site has been significantly reduced, which could hardly enhances H_2O adsorption and might lead to the inhibition on reaction rate. In general, these experimental results somehow illustrate the roles of the oxygen sites/vacancies played in the dissociation of chemisorbed H_2O molecule on CaO surface, and prove the reaction path and mechanism shown in Figure 4 a) and b) to certain extent.

4. Binding Energy of the Reactions Products

Figure 8 shows a distinct difference (about 0.25eV) of the Se3d binding energies from the reaction products with and without steam, which indicates that there exists different SeO_2 adsorptions on CaO surface under different reaction conditions. The peak position of binding energy without steam is consistent with previous researches [31].

The decrease of SeO_2 binding energy represents the decreases of the binding capacity of adsorption products, suggesting that SeO_2 molecule could be more easily chemisorbed in reactions. As shown in Figure 4 c), the mechanism proposed before also suggests that the adsorption capability for SeO_2 molecule on CaO surface might be promoted by CaO-Steam reaction products under appropriate temperatures. This assumption can be somewhat approved by Figure 8.

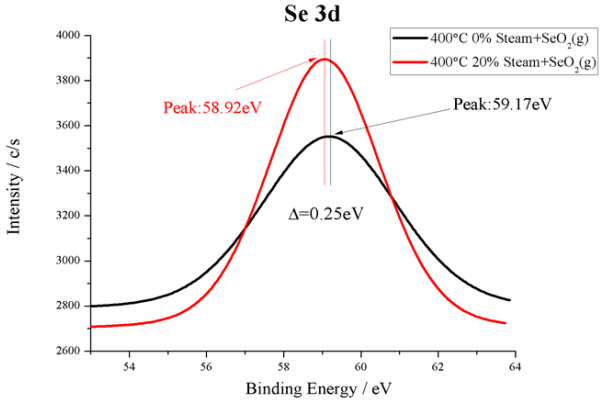

Figure 8. The Se3d binding energy of products.

The binding energies of Ca2p of three products obtained from different reaction conditions are shown in Figure 9. The results are listed in the descending order of the peak positions of Ca2p binding energy, i.e. CaO + 20% steam, CaO + 20% steam + gaseous SeO_2, and CaO + gaseous SeO_2 alone. The difference of peak position also indicates the different adsorption mechanisms, as suggested by Figure 8.

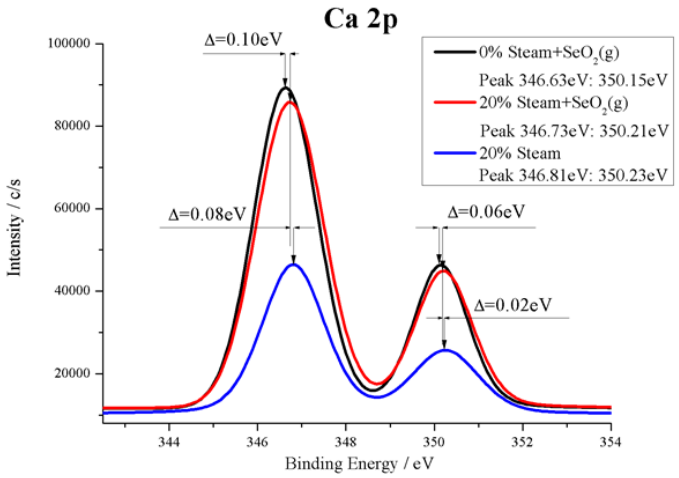

Figure 9. The Ca2p binding energy of products.

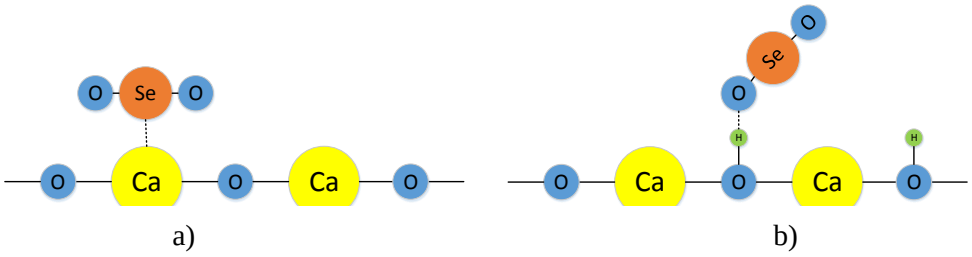

Figure 10. The structure for CaO adsorbing SeO_2 molecule: a) without steam, b) with steam.

The surface structure of CaO + 20% steam + gaseous SeO_2 may be described as Figure 10 b), which corresponds to the assumption in Figure 4 d), as indicated from the analysis of peak positions of Ca2p binding energies in Figure 9. The surface structure of CaO + 20% steam could be described as Figure 4 b), according to previous researches [22], [23]. Comparing with CaO + 20% steam, the peak positions of Ca2p binding energies of CaO + 20% steam + gaseous SeO_2 are very close to each other, indicating that Ca atom status are similar in these two cases. One reasonable explanation is demonstrated as Figure 10 b) for the condition of CaO + 20% steam + gaseous SeO_2.

The differences of the peak position of Ca2p binding energy shown in Figure 9 also illustrate that there are two totally different mechanism in CaO + 20% steam + gaseous SeO_2 and CaO + gaseous SeO_2. Due to the differences shown in Figure 9, the status of Ca atom is different, suggesting the different surface structure and different reaction mechanism. Fan et al. analysed the SeO_2 molecular adsorption processes on CaO surface without steam [32], [33]. From his work, the adsorption structure of CaO + gaseous SeO_2 could be presented as Figure 10 a), which is obviously different from Figure 10 b), i.e. the condition of CaO + 20% steam + gaseous SeO_2, and explains the difference of the peak positions of Ca2p binding energies in these two conditions.

5. Conclusion

The experimental study of this work illustrates that steam can promote CaO adsorbing SeO_2. Based on previous researches, the effect of oxygen vacancies on CaO surface is proposed as the main reason of the promotion as the dissociation of chemisorbed H_2O benefits SeO_2 adsorption. The mechanism is then verified by a set of specifically designed experiments and characterization of reaction products.

Main conclusions include: 1) For SeO_2 adsorption without steam, the adsorption ability of CaO surface positively related with temperature from 240℃ to 800℃; 2) In the experimental temperature and steam concentration range, steam could apparently promote the SeO_2 adsorption rate on CaO surface. Under relative low concentration, the promotion effect of steam is more recognizable; 3) From 240℃

to 800℃, steam could help CaO adsorb more SeO_2, the reaction rates curve has a peak at around 600℃; 4) The mechanism of the steam enhancing SeO_2 adsorption on CaO is similar to that of enhancing H_2O sorption as previous researchers indicated, similar as the role in carbonation of Calcium. Vacancy is dominant in the process of the dissociation of chemisorbing H_2O molecule on CaO solid surface and the hydroxyl groups formed from H_2O molecule is essential for SeO_2 adsorption. A series of designed experiments and reaction products characterization have confirmed the proposed mechanism.

6. Appendices

Nomenclature

Symbol	Description	Units
Vo	oxygen vacancy on CaO surface	-
Oo	oxygen atom on CaO surface	-
OHo	hydroxyl site on CaO surface which is exactly on oxygen site	-
$\mathbf{E_{H2O,\ diss,\ ad}}$	Activation energy of H_2O molecule dissolving and adsorption	kJ mol^{-1}
$\mathbf{E_{H2O,\ ad}}$	Activation energy of H_2O molecule adsorption	kJ mol^{-1}
$\mathbf{E_{OH,\ ad}}$	Activation energy of hydroxyl groups formed from H_2O molecular adsorption	kJ mol^{-1}
$\mathbf{E_{H,\ ad}}$	Activation energy of H adsorption	kJ mol^{-1}
$\mathbf{E_{H2O,\ diss}}$	Activation energy of H_2O molecule dissolving	kJ mol^{-1}
$\mathbf{SeO_2}$ Ⅰ	SeO_2 adsorption quantity during adsorption teat in with-steam experiments, determined by ICP-AES	μg
$\mathbf{SeO_2}$ Ⅱ	SeO_2 content in collected solutions, from dissolving the second-placed CaO solid and washing the exhaust gas collection system in with-steam experiments, determined by ICP-AES	μg
$\mathbf{C_{H2O}}$	steam concentration in with-steam experiments	%
$\mathbf{W_0}$	CaO sample weight after the Pretreatment Ⅰ	μg
W'	sample weight after 20min reaction in with-steam experiments	μg
$\mathbf{W_i}$	increment of sample weight in with-steam experiments	μg
$\mathbf{W_{SeO2}}$	SeO_2 weight in the sample determined by ICP-MS in with-steam experiments	μg
τ	Reaction duration in with-steam experiments	min
$\mathbf{R_0}$	The SeO_2 adsorption rate in without-steam experiments	μg/min

7. References

[1] Asokan P, Saxena M, and Asolekar S 2010 *Mater. Charact.* **61** 1342−1355.
[2] Wang L, Ju Y, Liu G, Chou C, Zheng L, and Qi C 2010 *Environ. Earth Sci*. **60** 1641-1651.
[3] Peng A, Wang Z, and Whanger P D 1995 *The environmental biology inorganic chemistry of selenium* (Beijing: Environmental Science Press of China) p156.
[4] Diehl S F, Goldhaber M B, Koenig A E, Lowers H A, and Ruppert L F 2012 *Int J. Coal Geol*. **94** 238.
[5] Zhu J, Johnson T M, Finkelman R B, Zheng B, Sykorova I, and Pesek J 2012 *Chem. Geol.* **330** 27−38.
[6] Pacyna E G, Pacyna J M, Sundseth K, Munthe J, Kindbom K, Wilson S, Steenhuisen F, and Maxson P 2010 *Atmos. Environ.* **44**(20) 2487-2499.
[7] Tian H, Wang Y, Xue Z, Qu Y, Chai F, and Hao J 2011 *Sci. Total Environ.* **409**(16) 3078-3081.
[8] Pacyna J M and Pacyna E G 2001 *Environ. Rev.* **9**(4) 269-298.
[9] Rosenberg W G 1991 *Sci. New Series* **251**(5001) 1546-1547.
[10] Rubin E S 1999 *Environ. Sci. Technol*. **33** 3062-3067.
[11] Li Y, Tong H, Zhuo Y, Chen C, and Xu X 2006 *Environ. Sci. Technol.* **40** 4306-4311.
[12] Li Y, Tong H, Zhuo Y, Wang S, and Xu X 2006 *Environ. Sci. Technol.* **40** 7919−7924.
[13] Xu S, Shuai Q, Huang Y, Bao Z, and Hu S 2013 *Energy Fuels* **27** 6880−6886.
[14] Ghosh-Dastidar A, Mahuli S, Agnihotri R, and Fan L S 1996 *Environ. Sci. Technol.* **30** 447-452.
[15] Agnihotri R, Chauk S, Mahuli S, and Fan L S 1998 *Environ. Sci. Technol.* **32** 1841-1846.

[16] Somoano D, and Martinez-Tarazona M R 2004 *Environ. Sci. Technol.* **38** 899−903.
[17] Dobner S, Sterns L, Graff R A, and Squires A M 1977 *Ind. Eng. Chem. Process Des.* **16** 479
[18] Donat F, Florin N H, Anthony E J and Fennell P S 2011 *Environ. Sci. Technol.* **46** 1262−1269.
[19] Manovic V and Anthony E J 2010 *Eng. Chem. Res.* **49** 9105–9110.
[20] Yang S J and Xiao Y H 2008 *Ind. Eng. Chem. Res*. **47** 4043−4048.
[21] Fennell P S, Pacciani R, Dennis J S, Davidson J F, and Hayhurst A N 2007 *Energy Fuels* **21**(4) 2072−2081.
[22] Li Z, Liu Y, and Cai N 2014 *Fuel* **127** 88-93
[23] R. Schaub, P. Thostrup, N. Lopez, E. Lægsgaard, I. Stensgaard, Noskov J K, and Besenbacher F 2001 *Phys. Rev. Lett.* **87** 266104.
[24] Carrasco J, Illas F, and Lopez N 2008 *Phys. Rev. Lett.* **100** 016101.
[25] Manzano H, Pellenq R J M, Ulm F J, Buehler M J, and Duin A C V 2012 *Langmuir.* **28** 4187-4197.
[26] Ochs D, Braun B, Maus-Friedrichs W, and Kempter V 1998 *Surf. Sci.* **417** 406-414
[27] Sterling R O and Helble J J 2003 *Chemosphere* **51** 1111-1119.
[28] Bhaskar D M, Gargi D, Umesh V W, and Hegde M S 2012 *Chem. Mater*. **24** 4491−4502.
[29] Wang Y, Yang X, and Li J 2016 *Chin. J. Catal.* **37** 193–198.
[30] Yang Z, Fu Z, Zhang Y, and Wu R 2011 *Ind. Eng. Catal. Lett.* **141** 7-82.
[31] Fan Y, Yao J G, Zhang Z, Sceats M, Zhuo Y, Li L, Maitland G C and Fennell P S 2018 *Fuel Process. Technol*. **169** 24-41.
[32] Fan Y, Zhuo Y, and Li L 2017 *Appl. Surf. Sci.* **420** 465-471.
[33] Fan Y, Zhuo Y, Lou Y, Zhu Z, and Li L 2017 *Appl. Surf. Sci*. **413** 366-371.

8. Acknowledgment

The authors gratefully acknowledge financial support from the National Natural Science Foundation of China (51776107).